"HENRI COANDA"
AIR FORCE ACADEMY
ROMANIA

"GENERAL M.R. STEFANIK"
ARMED FORCES ACADEMY
SLOVAK REPUBLIC

INTERNATIONAL CONFERENCE of SCIENTIFIC PAPER
AFASES 2012
Brasov, 24-26 May 2012

MATHEMATICAL MODELING FOR MELTED ZONE IN LASER WELDING FOR STEEL

Cristian MÎNZAT*, Remus BOBOESCU*

* Mechanical Faculty, University Politehnica, Timisoara, Romania,

Abstract: On the thick carbon steel plates were made welds with Nd:YAG laser beam. Weld width and crater obtained at stopping irradiation characterize the weld surface. It presents mathematical models that show the effect of power, welding speed and laser beam defocusing on these sizes. The hierarchy of effects by Pareto charts compares defocus effect to power and welding speed effects. Heat affected zone in on the weld cross section shows that the power has main roll in achieving melted in the material.

Keywords: *laser welding, weld crater, melt steel, laser beam defocus*

1. INTRODUCTION

Experiments consisted of fusion lines thick steel plates. Its will be called welds. Weld cross section showed the entire melted area inside material. The weld depth and melted area on weld cross-section are important for achieving welding joints.

The parameters variations were considered laser power, welding speed and defocusing in study [1]. Particular interest to defocus variations on the weld characteristics were reported in the paper [2]. As they use the laser focus within the piece. Laser focus over the piece was used in the work [3].

This paper studied several quantities that characterize the molten material obtained in irradiation with moving laser beam. Quantities that characterize the melt have been classified into two types, sizes related to weld surface and sizes related to weld cross section.

Analysis of these sizes was performed using Statgraphics program. It presents polynomial mathematical models of 3 degree to correlate objective function values (measured size) with parameter values .Statistical analysis of effects and interactions between parameters is given by ANOVA Analysis of variance.
Hierarchy of effects is presented by Pareto charts. Representations using the response functions show the variation of measured quantities with the variation of two parameters. These are customizations of mathematical models previously presented.

The aim of presented analysis is to highlight the effect of focus compared to that of power and welding speed. Laser melting effects are most easily revealed by sizes measured on the weld surface. Their variation was compared with the heat affected zone area, size measured on weld cross section.

2. EXPERIMENTS

The material used was steel Dillimax500 EN 10137. This is a fine grain steel with high elasticity limit. Chemical composition with upper limit expressed as a percentage is given as follows: $C \leq 0.16$, $Si \leq 0.5$, $Mn \leq 0.1.6$,

$P\leq 0.02$, $S\leq 0.01$, $Cr\leq 0.7$, $Ni\leq 1$, $Mo\leq 0.6$, $V+Nb\leq 0.08$

The experiment consisted of fusion lines (welds) with the line length of 110mm on steel Dillimax500 plates with 10 mm thickness. An industrial laser machine Nd: YAG Trumph Haas 3006D was used. It emits radiation with wavelength λ = 1.06 μm and have a maximum power of 3kW. Irradiation was performed in continuous regime. Laser beam was transmitted through a fiber with 0.6mm diameter. The focusing system assures the spot in focal point with 0.6mm diameter. The focal distance of lens was 200mm. As protective gas was argon with a flow rate of 20l/min. The welds were made on the sheets of material with $100\times 130\times 10$ mm dimensions. There was a space 20mm between two consecutive welds.

The radiation was controlled by variation of three parameters: laser power, welding speed and defocusing, Figure 1.

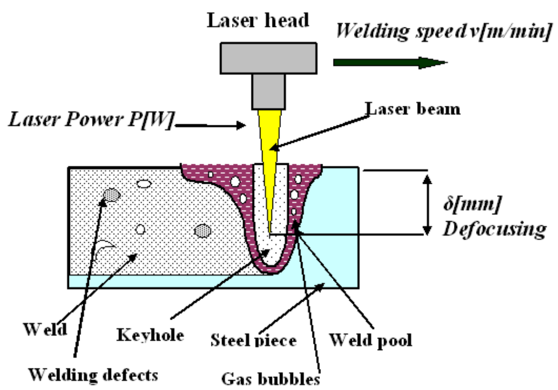

Figure 1 Schematic diagram of the laser welding process with varied parameters in experiments

After the welding the plates was cut. Cutting of plates was performed at 20 mm before the end of the process, in stabile part of weld, at same distance for all welds. The piece section has been metallographic processed (polishing and acid attack using Nital) to obtain images of melted metal, heat affected zone (HAZ), and microstructure, On the metallographic processed section were made measurements heat affected zone area A[mm^2].This was measured using a millimeter scale of precision 1 mm^2 on the weld cross-section.

The experimental plan used was one of complete factorial. To achieve mathematical models and statistical analysis of variations was used Statgraphics program.

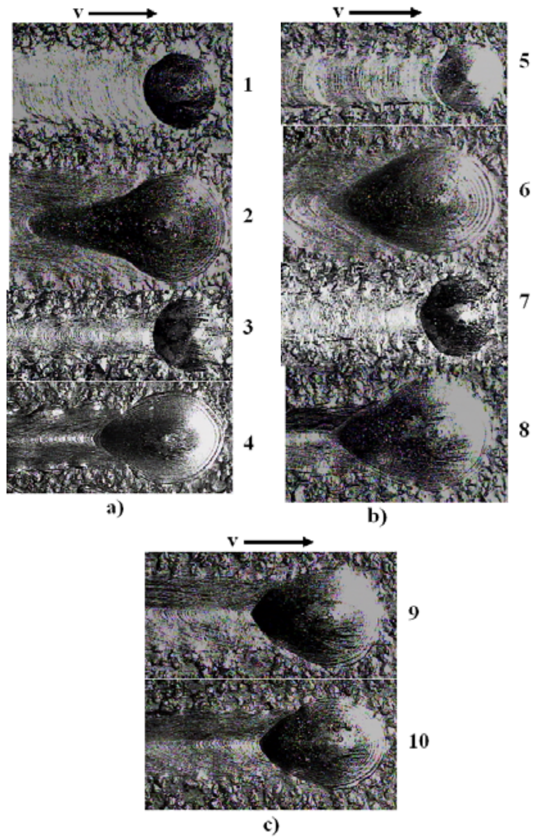

Figure 2 Photos of the crater produced at the end of the welding process a) focus at piece surface, b) focus within the piece c) replies

Table 1 Varied parameters values in experiment

Nr. crt.	Power		Welding speed		Defocusing	
	P[kW]	A[-]	v [m/min]	B [-]	δ [mm]	C [-]
1	1	-1	0,6	-1	0	-1
2	3	+1	0,6	-1	0	-1
3	1	-1	1,5	+1	0	-1
4	3	+1	1,5	+1	0	-1
5	1	-1	0,6	-1	-2	+1
6	3	+1	0,6	-1	-2	+1
7	1	-1	1,5	+1	-2	+1
8	3	+1	1,5	+1	-2	+1
9	2	0	1	0	-1	0
10	2	0	1	0	-1	0

For this analysis were introduced a dimensionless parameters values. Switching between the two systems of values of parameters is given by the following relations:

$$A = P - 2\ [\text{-}] \tag{1}$$

$$B = -2.33 + 2.22v\ [\text{-}] \tag{2}$$

$$C = -1 - \delta\ [\text{-}] \tag{3}$$

Both systems will be used for the presentation of mathematical models. Experimntal plan is presented in Table 1. Images of the surface of welds associated with the experimental plan are presented in Figure 2.

3. WELD WIDTH

The mathematical model for weld width L is given by the following relations:

$$L = 2.034 + 0.5825A - 0.46B + 0.0075C - 0.025AB + 0.2925AC - 0.085BC - 0.3ABC \quad [\text{mm}] \quad (4)$$

$$L = -0.70875 + 0.93075P - 2.0535v - 0.62245\delta + 0.6105Pv + 0.4065P\delta - 1.1433v\delta + 0.666Pv\delta \quad [\text{mm}] \quad (5)$$

Statistical analysis of the effects for weld width with ANOVA method is presented in Table 2

Table 2 ANOVA for weld width L

Effect	Sum of Squares	DF	Mean. Sq.	F-Ratio	P-val
A(power)	2.7144	1	2.7144	18.09	0.05
B(speed)	1.6928	1	1.6928	11.28	0.07
C(defocusing)	0.0004	1	0.0004	0.00	0.96
AB	0.0050	1	0.0050	0.03	0.87
AC	0.6844	1	0.6844	4.56	0.16
BC	0.0578	1	0.0578	0.39	0.60
ABC	0.7200	1	0.7200	4.80	0.15
Total error	0.3000	2			
Total (corr)	6.1750	9			
$R^2 = 0.95$			$R^2(adj.\,for\,d.f.) = 0.78$		

Figure 3 shows the Pareto chart for weld width. Power has the highest effect. The power effect is statistically significant. Welding speed has the effect opposite to power, which is the second effect. The third effect is the third order interaction between parameters. This is a decreasing effect. The decreasing effect is given by welding speed by itself effect and by interactions effect that involving welding speed. The high third order interaction effect covers interactions of order 2 and that of defocus effects. It is shown that for weld width welding speed effect is stronger.

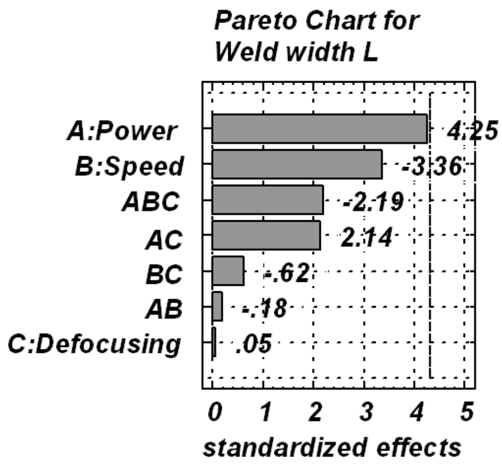

Figure 3 Pareto chart for weld width

Figure 4 shows that on the experimental field weld width increases with power and decreases with welding speed. Direct dependence of power and welding speed makes the weld width variation on the experimental to be almost linear.

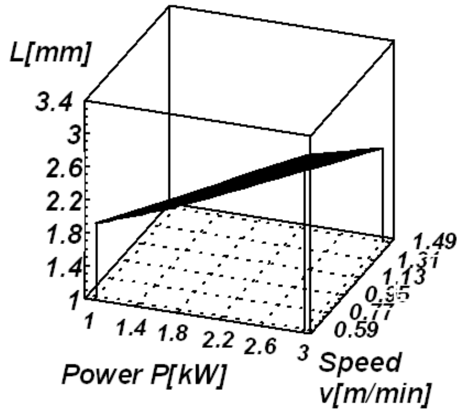

Figure 4 Variation of weld width with power and welding speed

4. CRATER AREA

The mathematical model for crater area acr is given by the following relations:

$$acr = 10.017 + 6.885.A + 2.2225.B + 0.665.C + 2.9325.AB + 1.3.AC - 0.8925.BC - 0.9075.ABC \quad [mm^2]$$
(6)

$$acr = -12.45445 + 14.5322P - 10.1343v - 0.214425\delta + 8.5248Pv + 0.814475P\delta - 2.04795 + 2.01465\,Pv\delta \quad [mm^2] \quad (7)$$

Figure 5 shows the Pareto chart for the crater area. Note that power has the highest effect on the crater area. All parameters have an increasing effect on the crater area. Decrease of crater area is given by the interaction between defocus and welding speed. This interaction is associated with a simultaneous decrease in the intensity of laser beam at piece surface and interaction time between laser and material, disadvantage both for melting and vaporization of the material. Presented effects have not statistically significance. The positive effect of welding speed can be explained by favoring the production of molten material against vaporization.

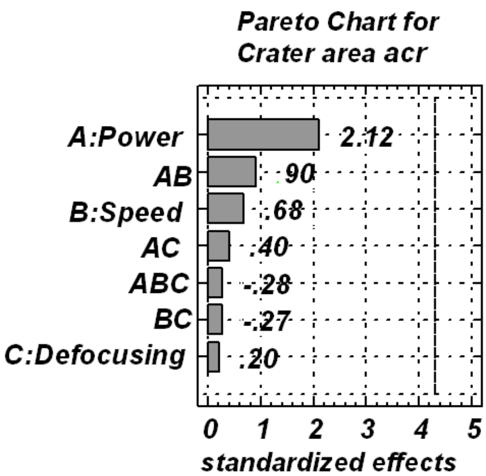

Figure 5 Pareto chart for crater area

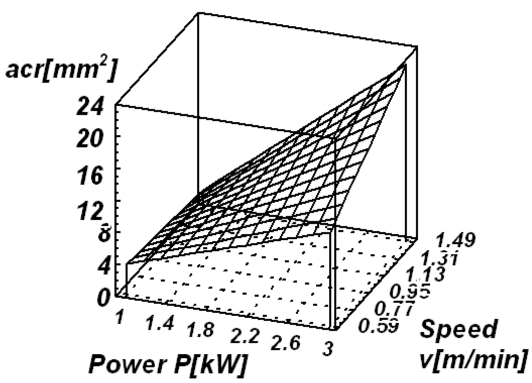

Figure 6 Variation of crater area with power and welding speed

Response surface of Figure 6 shows that on the experimental field crater area increases with power and welding speed. Increasing with the welding speed is stronger at higher power. It shows out so increasing the amount of melt in welding bath and increasing melt movement.

5. CIRCULARITY DEVIATION

The mathematical model for circularity deviation abc is given by the following relations:

$$abc = 57.16 + 45.9625.A - 16.1625.B - 16.2375.C - 11.3125.AB - 10.4375.AC + 14.0375.BC + 12.0375.ABC \quad [\%] \quad (8)$$

$$abc = -0.9575 + 1.9945P + 36.63v + 18.749875\delta - 51.837Pv - 17.609875\,P\delta + 22.28325v\delta - 26.72325\,Pv\delta \quad [\%] \quad (9)$$

Statistical analysis of the effects for circularity deviation with ANOVA method is presented in Table 3

Table 3 ANOVA for circularity deviation

Effect	Sum of Squares	DF	Mean. Sq.	F-Ratio	P-val
A(power)	16900.411	1	16900.411	63.60	0.01
B(speed)	2089.811	1	2089.811	7.86	0.10
C(defocusing)	2109.251	1	2109.251	7.94	0.10
AB	1023.781	1	1023.781	3.85	0.18
AC	871.531	1	871.531	3.28	0.21
BC	1576.411	1	1576.411	5.93	0.13
ABC	1159.211	1	1159.211	4.36	0.17
Total error	531.455	2	265.728		
Total (corr.)	26261.864	9			
$R^2 = 0.97$			$R^2(adj.for\,d.f.) = 0.90$		

Figure 7 shows the Pareto chart for the deviation from circularity of the crater. Power has the highest effect. Crater deformation has strong increase with power. Defocus and welding speed have the opposite effect of decreasing crater deformation. Decrease welding speed favor evaporation and thus decreases the amount of melt. Focus inside piece increases laser beam spot diameter and thus favors circular shape of the crater. Note that all effects presented were statistically significant. Note that the effect of parameters is greater than the effect of interactions between parameters.

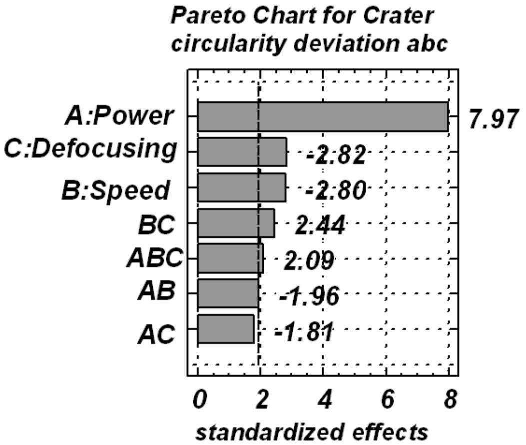

Figure 7 Pareto chart for circularity deviation

Response surface in Figure 8 shows the variation of deviations from circularity with power and welding speed. On the experimental field, crater deformation increases with power. At low power crater deformation increases with welding speed and at high power crater deformation decreases with welding speed.

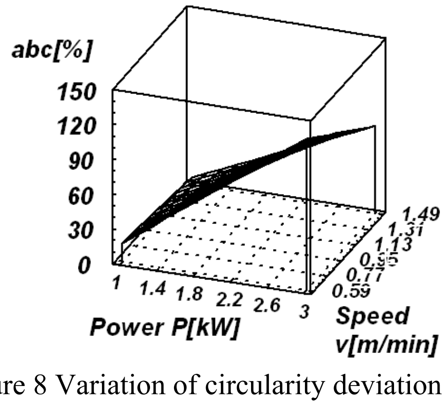

Figure 8 Variation of circularity deviation with power and welding speed

6. HEAT AFFECTED ZONE ON WELD CROSS SECTION

The mathematical model for heat affected zone area is given by the following relations:

$$A = 9.7 + 7.5A - 3.875B + 0.125C - 2.875AB + 0.625AC + 0BC + 0.25ABC \; [\mathrm{mm}^2] \quad (10)$$

Statistical analysis of the effects for heat affected zone area with ANOVA method is presented in Table 4.

Table 4 ANOVA for heat affected zone area

Effect	Sum of Squares	DF	Mean. Sq.	F-Ratio	P-val
A(power)	450.000	1	450.000	71.43	0.01
B(speed)	120.125	1	120.125	19.07	0.04
C(defocusing)	0.125	1	0.125	0.02	0.90
AB	66.125	1	66.125	10.50	0.08
AC	3.125	1	3.125	0.50	0.56
BC	0.00	1	0.00	0.00	1.00
ABC	0.50	1	0.50	0.08	0.80
Total error	12.60	2	6.30		
Total (corr)	652.60	9			
$R^2 = 0.98$			$R^2 (adj. for\, d.f.) = 0.91$		

Figure 9 shows the Pareto chart for the heat affected zone on the weld cross section. Note that the highest effect is power effect followed by the effect of the interaction between power and welding speed. Last effects are the defocusing effects and interactions involving it.

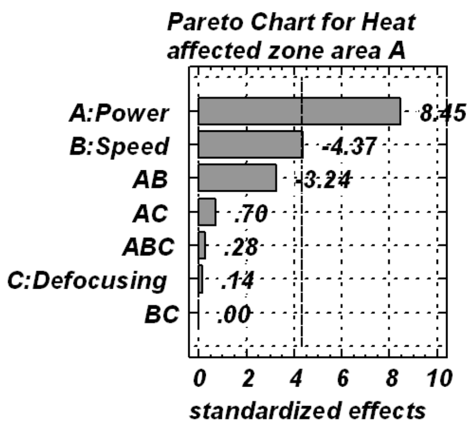

Figure 9 Pareto chart for heat affected zone area on weld cross section

Effects of power and welding speed were statistically significant. It is shown that defocusing role is reduced in determining the weld cross section melted area.

Response surface in Figure 10 shows the variation of heat affected zone area on the weld cross section with power and welding speed. It is noted that the area increases with power. Welding speed causes a significant decrease in case to use high power values.

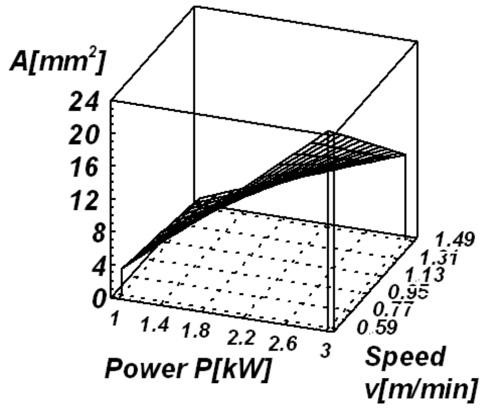

Figure 10 Variation of heat affected zone area with power and welding speed

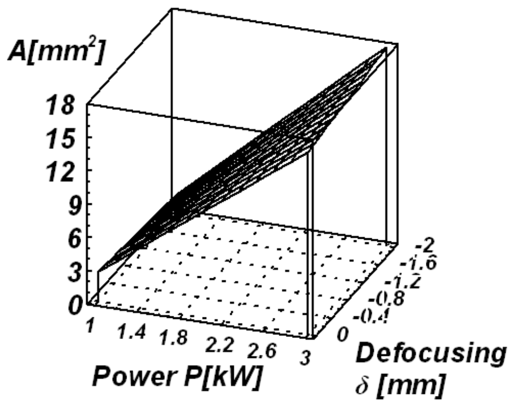

Figure 11 Variation of heat affected zone area with power and defocus

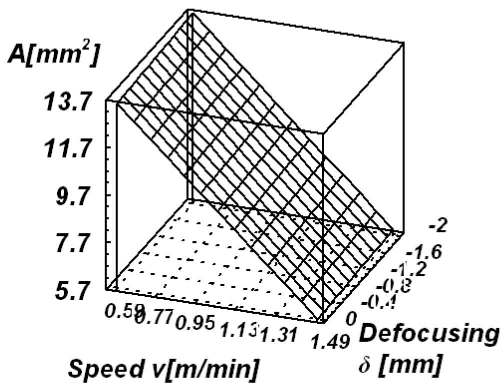

Figure 12 Variation of heat affected zone area with welding speed and defocus

Figure 11 presents the variation heat affected zone area with power and defocus. Note that on the experimental field heat affected zone area increases with power. Defocus does not produce significant variations. A linear type variation is obtained.

Figure 12 shows the variation for heat affected zone area according to the speed and defocus. Note that on the experimental heat affected zone area decreases with welding speed. Figures 11 and 12 shows that the variation of heat affected zone area with power and welding speed practically does not depend on defocus.

7. CONCLUSIONS

In the paper were presented mathematical models for sizes which characterize laser beam welds made on steel plates. There have been mathematical models that consider the parameters effects and interactions of the. We analyzed the molten zone on weld surface.

Has been shown that defocus produces variations on quantities which characterize the weld surface, but does not produce significant variations in material melted zone on weld cross section. This paper presents a mathematical model characterizing the variations of weld surface sizes based on a type 2^3 experimental plan.

From analyzed sizes mathematical models for deformation crater are appropriate and statistical significance.

REFERENCES

1. Abdel-Monem, El-Batahgy ,Effect of laser welding parameters on fusion zone shape and solidification structure of austenitic stainless steels, *Materials Letters 32* (1997) p:155-163
2. E. Akman, A. Demir, T. Canel, T. Sınmazcelik, Laser welding of Ti6Al4V titanium alloys *Journal of materials processing technology 209* (2009) p:3705–371
3. Rattana Borrisutthekul, Yukio Miyashita, Yoshiharu Mutoh Dissimilar material laser welding between magnesium alloy AZ31B and aluminum alloy A5052-O *Science and Technology of Advanced Materials xx* (2005) p:1–6.